#### **Supplementary Information**

#### **Supplementary Materials and Methods**

#### Immunohistochemistry

The primary antibodies were used at the following dilutions: mouse anti-FOXA1 (WMAB-2F83, 1:1,000; Seven Hills); goat anti-FOXA2 (sc-6554, 1:250; Santa Cruz); goat anti-HNF4α (sc-6556, 1:200; Santa Cruz); rabbit anti-PROX1 (11-002P, 1:200; Angiobio); rabbit anti-cleaved-CASPASE3 (ab13847, 1:250; Abcam); rabbit anti-PDX1 (ab47267, 1:1,000; Abcam); guinea pig anti-PDX1 (ab47308, 1:1,000; Abcam); rabbit anti-pH3 (ab5176, 1:500; Abcam); rabbit anti-SOX9 (AB5535, 1:1,000; Millipore); mouse anti-SOX9 (ab76997, 1:500; Abcam); rabbit anti-pSMAD1/5/9 (13820S, 1:200; Cell Signaling Technologies), mouse anti-SMA (A2547, 1:1,000; Sigma); rabbit anti-hrGFP (240142-51, 1:500; Stratagene Vitality); SOX17 (AF1924, 1:500; R&D Systems). The secondary antibodies used were Alexa Fluor 488, 546 or 647 (1:500, Molecular Probes).

#### Section In Situ hybridization

Section in situ hybridization was performed as described in the materials and methods section of the main text using Bmp2 (1), Bmp4 (2) and Bmp7 (3). For Alk3, Alk2 and Bmpr2, probes were made using the primers listed below. The probe sequence was amplified from E9.5 embryonic cDNA. The amplified PCR products were cloned into the 4-TOPO Vector using the TOPO TA Cloning Kit (Invitrogen) according to manufacturer's instructions. The primers used for amplifying probe sequences are: Alk3 (forward) 5' CAGGACCAGTCATTCAAAGG 3', (reverse) 5' TCCAAATCACGGTTGTAACG 3': Alk2 (forward) 5' ACGGCTTTCCAACACATCACC 3', (reverse) 5' CAACAGGGTTATCTGGCGAGC 3'; Bmpr2 3', 5' (forward) 5' GCAGGATAAATCAGACGAAGAGC (reverse)

#### AATGAATGAGGTGGACTGAGTGG 3'.

#### Plasmid construction and transfection of Hepa1-6 cells or Hela cells

Dominant negative (dn) Alk3 (4) or dominant negative (dn) Alk2 (5) were cloned into the IREShrGFP2 expression vector (Vitality) at the BamH1 and the EcoR1 sites to obtain the dnAlk3hrGFP or the dnAlk2-hrGFP vectors that co-express hrGFP and dnAlk3 or hrGFP and dnAlk2 respectively. Sox9 was amplified from pWPXL-Sox9 (Addgene) using primers forward 5' ATGAATCTCCTGGACCCC 3' and reverse 5' GGGTCTGGTGAGCTGTGTG 3' and cloned into the IRES-hrGFP2 expression vector at the BamH1 and the EcoR1 sites to obtain the Sox9hrGFP plasmid that co-expresses hrGFP and Sox9. The IRES-hrGFP2 vector expressing only hrGFP was used as the control plasmid. The effectiveness of the expression plasmids to produce the respective functional proteins was first tested in Hepa1-6 cells for dnAlk3-hrGFP and Sox9-hrGFP and in Hela and U2OS cells for dnAlk2-hrGFP. Cells were thawed and passaged at least once to reach 80-90% confluency and then transfected with the respective plasmids (dnAlk3-hrGFP, dnAlk2-hrGFP, Sox9-hrGFP or hrGFP) using lipofectamine reagent (Thermo Fisher Scientific) following the manufacturer's protocol. Transfected cells were grown for 24 h and either used for Western blotting (below) or imaged for GFP to assess relative transfection efficiency. Transfections and corresponding western blots were performed at least twice as different biological replicates.

#### Western Blotting

Western blots were used to detect the presence of pSMAD1/5 in either cultured DMH1 treated or control embryos or in transfected tissue culture cells. Cultured embryos were pooled in groups of 3 and homogenized in a Dounce homogenizer followed by lysis in 100µl of RIPA buffer. Transfected cells were grown in 6-well plates and cells from each well were lysed in 100µl of RIPA buffer. The concentration of the protein obtained after lysis, was measured using the Bradford assay and approximately  $30\mu$ g of protein loaded onto each lane. Blots were probed with anti-pSMAD1/5 (9516S, 1:200; Cell Signaling Technologies) and anti-GAPDH (MAB374, 1:2,000; Millipore) for normalization. Anti-p44/42 MAPK (4376S, 1:1,000; Cell Signaling Technologies) and anti-Smad1/5 (sc6201, 1:500; Santa Cruz) were the other controls used. For cells expressing *Sox9-hrGFP*, blots were also probed with anti-FLAG M2 (F3165, 1:5,000; Sigma) to detect the presence of SOX9. Western blot band intensities were measured and normalization addressed using ImageJ software.

#### **Supplementary References**

1. Lyons KM, Pelton RW, Hogan BL. Patterns of expression of murine Vgr-1 and BMP-2a RNA suggest that transforming growth factor-beta-like genes coordinately regulate aspects of embryonic development. Genes Dev 1989;3:1657-1668.

 Jones CM, Lyons KM, Hogan BL. Involvement of Bone Morphogenetic Protein-4 (BMP-4) and Vgr-1 in morphogenesis and neurogenesis in the mouse. Development 1991;111:531-542.

3. Lyons KM, Hogan BL, Robertson EJ. Colocalization of BMP 7 and BMP 2 RNAs suggests that these factors cooperatively mediate tissue interactions during murine development. Mech Dev 1995;50:71-83.

4. Suzuki A, Thies RS, Yamaji N, Song JJ, Wozney JM, Murakami K, Ueno N. A truncated bone morphogenetic protein receptor affects dorsal-ventral patterning in the early Xenopus embryo. Proc Natl Acad Sci U S A 1994;91:10255-10259.

5. Luo J, Tang M, Huang J, He BC, Gao JL, Chen L, Zuo GW et al. TGFβ/BMP Type I receptors ALK1 and ALK2 are essential for BMP9-induced osteogenic signaling in mesenchymal stem cells. J Biol Chem 2010;285:29588-29599.

#### **Supplementary Figures**

Figure S1: Effectiveness of DMH1 in whole embryo culture. (A) The lysate of embryos dissected at 4-6S and subjected to whole embryo culture with or without DMH1 for 4, 8 or 12 h was used for Western blotting and probed with anti-pSMAD1/5, anti-SMAD1/5 (control), anti-pMAPK (pERK1/2) (specificity control) and anti-GAPDH (loading control). Quantified pSMAD1/5 band values were normalized to GAPDH and each treatment group compared as a fraction of the control. (B) Immunofluorescence on transverse sections illustrating the reduction of pSmad1/5/8 after 10 h of culture with DMH1 (n = 3). The yellow dashed lines mark the anterior hepatic endoderm. (C) Representative images of a dissected embryo (4-7S) prior to culture and after DMH1 or DMSO (vehicle) exposure at the end of culture (E9.25; 26-28h). The scale bar =  $50 \mu$ M.

Figure S2: Illustrations and representative images of sectioned mouse embryos. A and B) Illustrations (above) designed to define the orientation of sectioned images used throughout the paper. (A) Whole-mount depiction of a frontal view of an E8.5 embryo. The hepatic endoderm is colored red in depictions of transverse anterior (i) and posterior (ii) sections through the developing liver bud. Immunofluorescence for FoxA2 (red) highlights the endoderm and DAPIstained nuclei (blue) in anterior and posterior liver bud sections. (B) A whole-mount illustration of an E9.25 embryo and illustrations of sagittal sections through middle (iii) and lateral (iv) portions of the developing liver bud (red). Immunofluorescence of sections through whole E9.25 embryos using an HNF4 $\alpha$  antibody (green) to highlight hepatoblasts and DAPI counterstaining (blue) to view the entire embryo in representative middle sagittal and lateral sagittal sections. Figure S3: Inhibition of BMP signaling does not affect endodermal gene expression. A) Hematoxylin and eosin (H&E) staining of sagittal sections from control and DMH1 treated embryos cultured through E9.25. The upper and lower panels are the same except that the lower panels are marked: the STM boundaries are shown in black lines (indicated by white dotted lines in the main figures and other supplementary figures). The posterior hepatic domain (indicated by the blue dashed line) is that bounded by the STM while the anterior hepatic domain (outlined by the yellow dashed line) is that bounded by the SV. (B-D) Immunofluorescence of the endodermal markers FOXA1 and FOXA2 (B, C) and the hepatopancreatobiliary marker PROX1 (D) performed on lateral and medial sagittal sections of the hepatic region from control and DMH1 treated embryos. Although the liver buds of the drug treated embryos are noticeably smaller, no marker expression differences are noted between DMH1 treated embryos and controls. The number of embryos (n) analyzed in each control and treatment group is indicated on the right side of panel. Each scale bar = 50  $\mu$ M. SV = sinus venosus, STM = septum transversum mesenchyme.

### Figure S4: BMP is required for liver specification and maintenance between 4-18S stages.

A-D) To tease out the developmental window over which application of DMH1 perturbs liver specification and development, immunofluorescence of sagittal sections from cultured embryos treated with DMH1 at different stages was performed. (A) A significant loss of HNF4 $\alpha$  in the posterior liver bud is detected when cultures are started at the 10-12S. (B-C) When DMH1 is applied at the 13-15S and the 16-18S stages, a less severe phenotype is observed with a progressive reduction in the loss of HNF4 $\alpha$ + posterior liver bud region. (D) When the drug is applied at the 19-21S stages, no noticeable changes are observed compared with controls. The number of embryos (n) analyzed in each group is indicated on the right side of panel. Each scale bar = 50  $\mu$ M. The annotations are as in Figure S3.

Figure S5: BMP inhibition does not affect cell death or proliferation in the hepatic endoderm. A-C) Immunofluorescence of sections from control and DMH1 treated cultured embryos. Apoptosis was assessed in sagittal sections of E9.25 embryos (A) and in transverse sections of E8.5 embryos (B) using cleaved-CASPASE3 (CAS3). Little cell death is observed in HNF4 $\alpha$ + cells at the end of 26-28h of culture (A) nor in the early hepatic domain (outlined with yellow and blue dashed lines) 6 hours after culture (B). Cell proliferation was assessed in sagittal sections of E9.25 embryos (C) using pH3. (D) The rate of hepatoblast proliferation was determined as the ratio of cells expressing both pH3 and HNF4 $\alpha$  / the total number of cells expressing HNF4 $\alpha$  in the liver bud in either control or DMH1 treated embryos. The anterior and posterior regions of the lateral and middle liver bud were assessed. Although a trend of increased proliferation rate is observed in drug treated embryos versus control, there is no statistical significance. The number of embryos (n) analyzed in each control and treatment group is indicated within or on the right side of panel. Error bars in the graph represent standard deviation. Each scale bar = 50  $\mu$ M. Annotations are as in Figure S2. Lat = lateral, Ant = anterior, Pos = posterior, Mid = middle.

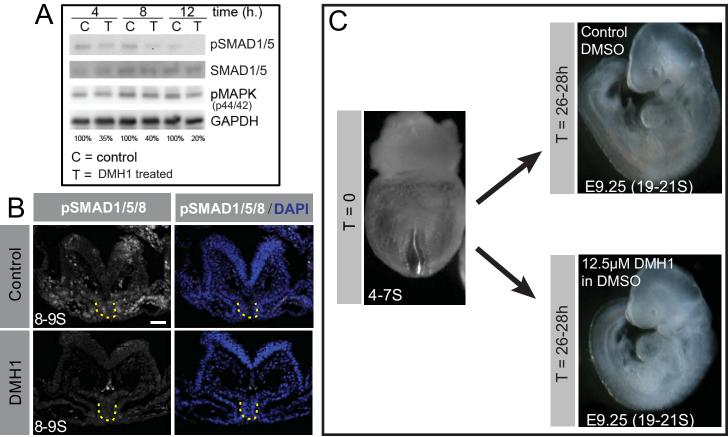
Figure S6: Normal distribution of labeled VMEL derivatives upon BMP inhibition. Control or DMH1 treated embryos were Dil-labeled (red) and cultured. Frontal view of the whole embryo shows Dil labeled VMEL progenitors at the onset of culture (E8.25). Section immunofluorescence after culture (E9.25) confirms that VMEL derivatives are present normally in the DMH1 treated embryos similar to controls. The number of embryos (n) analyzed in each control and treatment group is indicated on the right side of panel. Each scale bar = 50  $\mu$ M. Annotations are as in Figure S3.

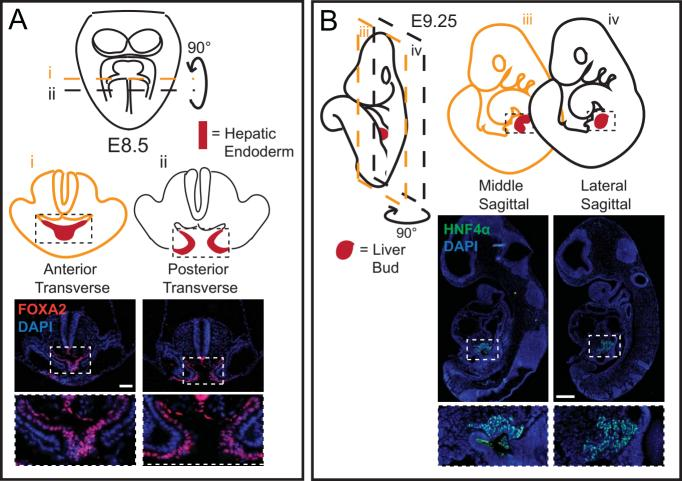
## **Figure S7: Construction and testing of the SOX9 expression plasmid in Hepa1-6 cells.** A) A graphic representation of the *Sox9-hrGFP* plasmid. (B) Bright-field (BF) or GFP fluorescence was monitored in Hepa1-6 cells transfected with either the *hrGFP* plasmid or the *Sox9-hrGFP* plasmid. (C) Western blot analysis of *hrGFP* and *Sox9-hrGFP* transfected cells probed with anti-FLAG (to detect SOX9) and anti-GAPDH (loading control). Each scale bar = 100 $\mu$ M.

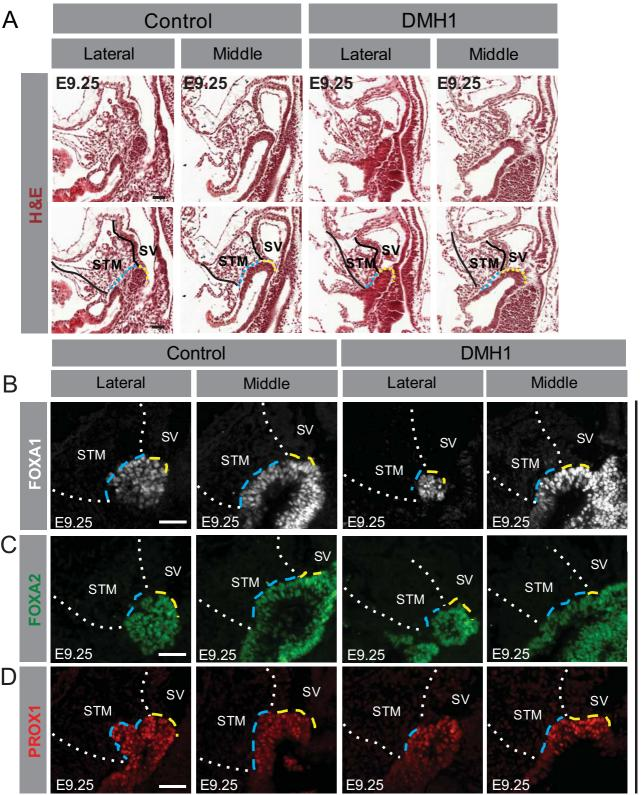
# Figure S8: Expression of BMP ligands and receptors during hepatic induction. A-F) Section in situ hybridization performed at the indicated stage with the BMP ligand or receptor probe listed. At 3-6S, the two lateral/posterior pre-hepatic endoderm progenitors are outlined by blue dashed lines in transverse sections. In transversely sectioned 8-10 and 11-12S embryos, the newly induced anterior and posterior liver bud are outlined by yellow and blue dashed lines, respectively. Lateral and medial sagittal sections of the newly internalized anterior (yellow dashed lines) and posterior (blue dashed lines) liver bud are displayed at 14-15S. Because BMP signals are required for anterior mesoderm derivatives including heart and allantois. transverse sections of both tissues at 11-12S embryos are provided as controls. (A) Bmp2 is present in the SV from 8-15S. By 14-15S Bmp2 is apparent in the STM. At 11-12S Bmp2 is present in the allantois, amnion and regions of the heart. (B) Bmp4 is neither expressed in the presumptive hepatic endoderm nor surrounding mesoderm prior to 14S. In the 14-15S embryo Bmp4 is detected in the anterior STM. Bmp4 expression is detected in the allantois and heart of 11-12S embryos. (C) Bmp7 is present in the hepatic endoderm and in the surrounding mesenchyme throughout early liver development. (D) Alk3 is weakly expressed in the hepatic endoderm between 3-12S and is upregulated in the 14-15S liver bud. (E) Alk2 is weakly expressed in the hepatic endoderm throughout liver development. (F) Bmpr2 is not expressed in the hepatic endoderm prior to induction but is weakly expressed in the hepatic endoderm beginning at 11-12S. Arrowheads highlight positive expression in the endoderm. The allantois is

indicated by pink asterisks. Annotations are as in Figure S3.

Figure S9: Construction of vectors expressing dominant negative (dn) *Alk3* and dominant negative (dn) *Alk2*. A) A graphic representation of the *dnAlk3-hrGFP* and the *dnAlk2-hrGFP* plasmids. (B and D) Bright field (BF) and GFP fluorescence was monitored in Hepa1-6 (B) or Hela (D) cells transfected with either *hrGFP* or *dnAlk3-hrGFP* (B) or *dnAlk2-hrGFP* (D) plasmids. (C and E) Western blot analysis of the cells in B and D with anti-pSMAD1/5, anti-p44/42 MAPK (specificity control) and anti-GAPDH (loading control). The pSMAD1/5 and GAPDH bands were quantified using ImageJ software and the values reported as percentages after normalization with loading control (bottom of each lane of the blots). Expression of *dnAlk3* (C) or *dnAlk2* (E) in cells leads to a reduction in pSMAD1/5 levels compared to cells expressing the *hrGFP* construct. The percent reduction (44% in C and 46.5% in E) roughly corresponds to the transfection efficiency in B and D respectively. Each scale bar = 100  $\mu$ M.







n = 3

